Perceptually Correct Haptic Rendering in Mid-Air Using Ultrasound Phased Array

Ahsan Raza, Waseem Hassan, Tatyana Ogay, Inwook Hwang, and Seokhee Jeon

***Abstract*—This paper provides a perceptually transparent rendering algorithm for an ultrasound-based mid-air haptic device. In a series of experiments, we derive a systematic mapping function relating from the device command value to final user's perceived magnitude of a mid-air vibration feedback. The algorithm is designed for the ultrasonic mid-air haptic interface that is capable of displaying vibro-tactile feedback at a certain focal point in mid-air through ultrasound phased array technique. The perceived magnitude at the focal point is dependent on input parameters, such as input command intensity, modulation frequency, and position of the focal point in the work-space. This algorithm automatically tunes these parameters to ensure that the desired perceived output at the user's hand is precisely controlled. Through a series of experiments, the effect of the aforementioned parameters on the physical output pressure are mapped, and the effect of this output pressure to the final perceived magnitude is formulated, resulting in the mapping from the different parameters to the perceived magnitude. Finally, the overall transparent rendering algorithm was evaluated, showing better perceptual quality than rendering with simple intensity command.**

***Index Terms*—Contact-less haptics, force feedback, haptic perception, mid-air haptic feedback, psychophysics.**

I. Introduction

ANALOGOUS to vision perception where reflected light energy is sensed by light-sensitive membrane in the eyes, humans perceive haptic information by sensing physical, i.e, mechanical/thermal/chemical, energy through the respective sensors underneath the skin [1]. A haptic interface should synthetically generate this physical energy and deliver them to the user's target body part. In general, these haptic related physical signals take mechanical coupling as a delivery medium, and thus, conventional haptic interface requires direct mechanical attachment to the user's body part, e.g., holding a pen-type interface [2], wearing a device [3], and an encountered-type interface. This constraint often introduces usability issues and becomes one of major hurdles in many applications.

To overcome this, many researchers are focusing toward providing contact-less force feedback in mid-air where the physical energy is delivered to the user's skin through air, so no direct attachment or coupling is needed to the user [4]. Three different technological approaches exist. One promising way is to use a laser as a medium of energy transfer in the air [5]. This approach is in its very early stage, and many practical issues, such as safety concerns, are still to be solved. Another approach uses air vortex to convey the energy in the air [6]. This is the simplest way, but the variety of feedback is limited. Another emerging technology is to use ultrasonic waves to transfer haptic-related energy. By controlling the phase of ultrasound waves from an array of ultrasonic transducers, the device can generate a focused acoustic radiation pressure at an arbitrary point on user's skin [7]. This approach has become an active research area due to significant advantages over other technologies, such as scalability and relatively simpler hardware setup. Many laboratory prototypes and semicommercial products have been developed, e.g., [8]–[10].

Main research focus of ultrasonic-based haptic device has been on the enhancement of physical characteristics of rendered pressure, e.g., increased strength, more focused pressure area, and enlarged work-space [8], [11]. Thanks to these efforts, it is considered that the quality of current implementations of the concept is quite at the level of practical application, and the quantitative physical performances are somewhat saturated. Thus, it is natural that the focus is moved to the perceptual performance of the feedback.

As one of the first step in this line of research, this paper is concerned with a perceptually accurate rendering algorithm specially designed for ultrasound-based haptic interfaces. Our algorithm takes the physical characteristics of the device into account. Due to the nature of phased-delay focus control, perceptual characteristics of the finally rendered pressure change not only as command intensity of the transducer changes, but also as modulation frequency, distance from the transducer array, and lateral position of the focal point in the work-space change. Thus, it is not a trivial task to generate perceptually

Manuscript received October 31, 2018; revised February 20, 2019; accepted March 18, 2019. Date of publication April 15, 2019; date of current version August 30, 2019. This work was supported in part by the Electronics and Telecommunications Research Institute grant funded by the Korean government under Grant19ZS1300 (The development of smart context-awareness foundation technique for major industry acceleration) and in part by the MSIP through IITP under Grant 2017-0-00179 (HD Haptic Technology for Hyper Reality Contents). *(Corresponding author: Seokhee Jeon.)*

A. Raza, W. Hassan, and T. Ogay are with the Department of Computer Science and Engineering, Kyung Hee University, Yongin-si 17104, South Korea (e-mail: ahsanraza@khu.ac.kr; waseem.h@khu.ac.kr; ta.ogay92@gmail.com).

I. Hwang is with the Smart UI/UX Device Research Section, Electronics and Telecommunication Research Institute, Daejeon 34129, South Korea (e-mail: inux@etri.re.kr).

S. Jeon is with the Department of Computer Science and Engineering, Kyung Hee University, Yongin-si 17104, South Korea (e-mail: jeon@khu.ac.kr).

Color versions of one or more of the figures in this paper are available online at http://ieeexplore.ieee.org.

Digital Object Identifier 10.1109/TIE.2019.2910036

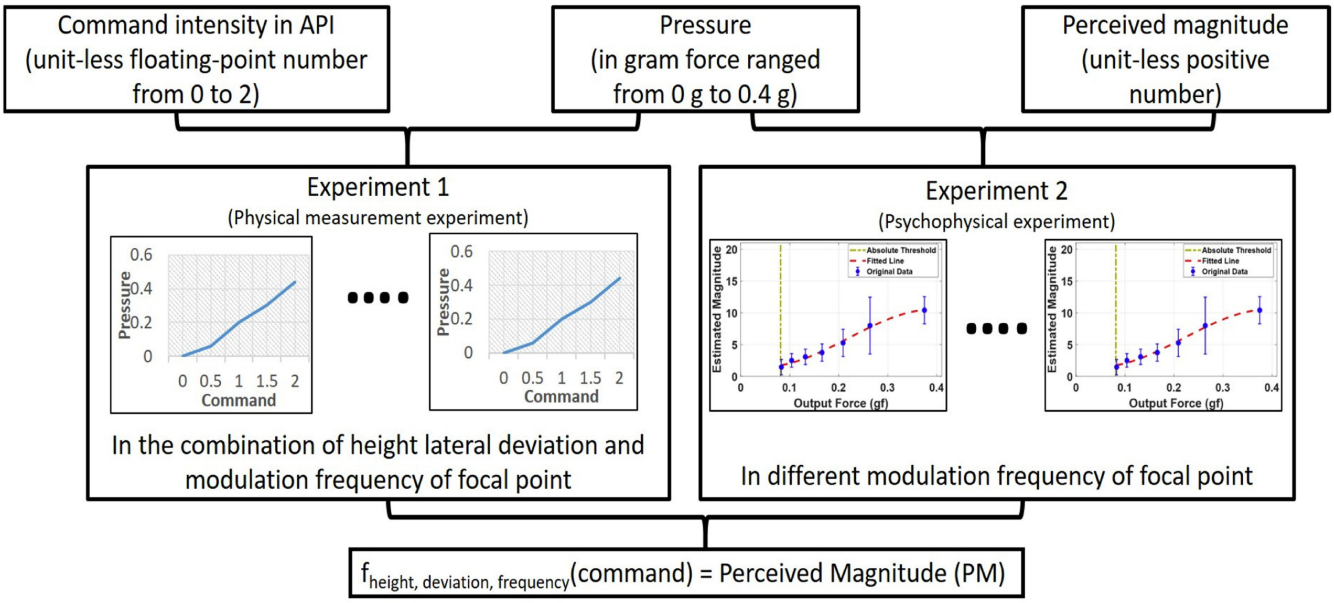

Fig. 1. Concept diagram: mapping from command to perception.

stable feedback under different situation. In this paper, we tried to empirically find a function connecting these parameters to perceptual strength of the feedback. This function plays a core role in rendering; the inverse of the function gets desired perceived magnitude and returns command intensity under a given frequency, height, and lateral position. This process can minimize the effect of device dynamics and allows us to solely focus on the final stimuli in feedback design.

This paper is motivated by the work done by Ryu *et al.* in [12]. They proposed a perceptually transparent rendering algorithm for vibrotactile feedback. In their work, input parameters of vibrations, i.e., modulation frequency and amplitude, are experimentally mapped to associated perceived magnitude, and then the mapping is used in rendering for perceptually accurate feedback. While the conceptual idea is similar, this paper takes a different approach for constructing the mapping, due to increased number of parameters; four inputs in our case, while two inputs in [12]. Instead of directly deriving the mapping, for each modulated frequency, we first connect the inputs to the generated pressure, and then the pressure is related to perceived magnitude. This two-step mapping allows us to avoid nearly infinite number of input parameter combinations for the experiment.

Another benefit of the approach is that it allows to separate the experiment into a physical measurement one and a psychophysical user study. This separation minimizes the amount of effort required for different ultrasonic haptic devices since the only device-dependent step is the first one, and thus, the time-consuming user-involved psychophysical experiment can be avoided. In this paper, we used the mid-air haptic display acquired from the company UltraHaptics to conduct the research [10].

The rest of this paper is organized as follows. The experiments carried out during this study and their results are detailed in Sections III and IV. Steps to implement the transparent rendering algorithm are explained in Section V. Evaluation performed is detailed in Section VI. In Section VII, we provide a detailed discussion based on the results of the experiments. Section VIII concludes this paper.

II. Overview

The goal of this paper is to build a framework that allows us to precisely control perceived strength of the pressure. To this end, two different experiments are conducted (see Fig. 1).

Experiment 1 establishes UltraHaptics device's physical characteristics. The original software application programming interface (API) provided in UltraHaptics device allows us to control the pressure intensity, the number, and the position of focal points. In this paper, we focus on the pressure intensity. The API takes normalized intensity value (0–2) coded in the program, which corresponds to a physical strength of the transducer output. As the air wave energy dissipates as it flies in the air, same transducer output strength cannot guarantee the same air pressure in different location of the focal point. In addition, different modulation frequencies affect the output pressure differently. Eventually, without exact mapping from the command intensity value to the proximal stimuli rendered at the users finger, precise rendering cannot be guaranteed. Note that simulation of the pressure in different location and frequency is a challenging task due to the complex nature of the phenomenon. Thus in Experiment 1, we empirically establish the relationship by formulating the effect of the height, lateral displacement of a focal point, and rendered frequency on the mapping between command intensity value and the magnitude of rendered pressure. As a unit of pressure, we used gram force (gf) under the assumption of uniform area of pressure application.

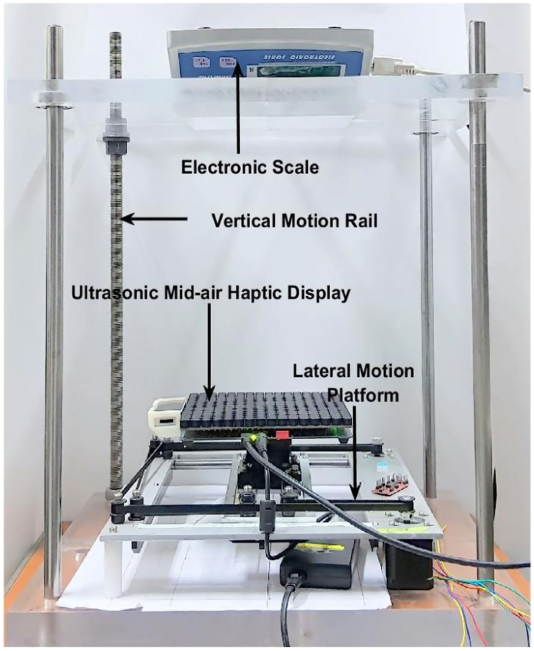

Fig. 2. Measurement system used to render the focal point and record its strength.

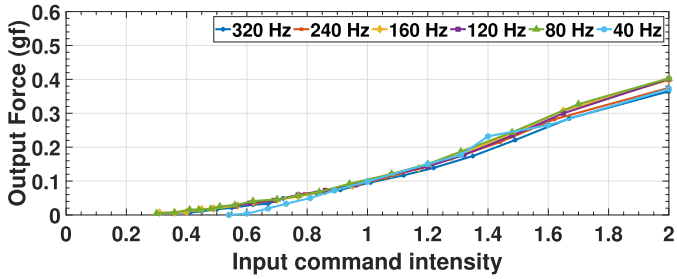

Fig. 3. Relation between input command intensity and the output gf.

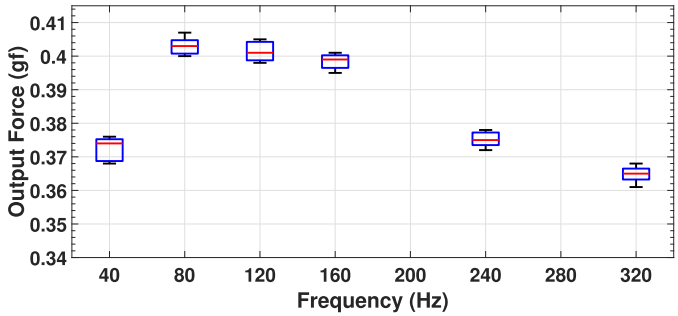

Fig. 4. Output pressure depending on the frequency, measured at the center with height of 250 mm.

Experiment 2 is a psychophysical experiment. It is well-known that humans have different sensitivity to vibrations with different frequencies due to the characteristics of the mechanoreceptors [13]. Hence, the perceptual precision of the rendering further guaranteed if this frequency effect is considered in rendering algorithm. To this end, through a series of psychophysical experiments we empirically found the absolute threshold (AL) and the supra threshold characteristics depending on rendered pressure in gf and frequency.

By combining the two, the whole route from the command intensity to the perceived magnitude is constructed and can be considered as a function taking command intensity and returning perceived magnitude. The inverse of this function enables the other way around; stimuli designer determines the desired magnitude in perceptual scale, and then the command intensity value (used in the API) is calculated in real time. Following Sections III and IV, detail the procedures and results.

III. Experiment 1

A. Measurement Hardware and Procedure

A measurement system, shown in Fig. 2, was designed to gauge the air pressure in gf at a focal point with different conditions. The air pressure was measured using a weight scale (the measurement resolution of the scale is 1 mg). A two-dimensional (2-D) motion platform was manufactured and used to precisely and systematically control the ultrasonic haptic device in the xy plane, while the height of the weight scale was adjusted by moving the z-stage.

Using the measurement system, the rendered pressure at the focal point is captured with different API's command intensity, the height of the focal point, the lateral deviation of focal point from the center, and rendered frequency of the focal point. The pressure measurement was done by recording five samples for each data point. Each sample was measured by presenting the focal point on the surface of weight scale for 5 s. The final results were computed after taking the average of all the samples for each data point.

B. Effect of Command Intensity and Frequency

We first see the effect of command intensity on the rendered pressure. In order to generate a trend, we fixed the position of the focal point (the height: 250 mm, lateral position: center). Data points were recorded for six different frequencies (40, 80, 120, 160, 240, and 320 Hz) and the input command intensity values of the device were varied from 0 to 2 with a step size of 1 dB between two consecutive values.

The recorded data are shown in Fig. 3. It can be seen that the command intensity and the pressure have a highly nonlinear relationship. It can also be seen that the magnitude of the pressure slightly decreases with increasing frequency. The sole effect of frequency is shown in Fig. 4. Further interpolation of the sample points is conducted using second order polynomials, which will be used to establish the transparent rendering algorithm. The generic equation for the polynomial model is provided in (1) and the fitted parameters for each frequency are presented in Table I.

$$\mathrm{gf}_i = M_i I^2 + N_i I + O_i \tag{1}$$

where gf is the gram force and I is the corresponding input intensity of the device. M, N, and O are the coefficients of the

TABLE I
SECOND-ORDER POLYNOMIAL COEFFICIENTS FOR (1)

i [Hz]	M_i	N_i	O_i	R_i^2
320	0.076	0.079	-0.049	0.98
240	0.073	0.090	-0.049	0.97
160	0.083	0.089	-0.056	0.99
120	0.097	0.046	-0.030	0.98
80	0.103	0.034	-0.019	0.99
40	0	0.28	-0.171	0.97

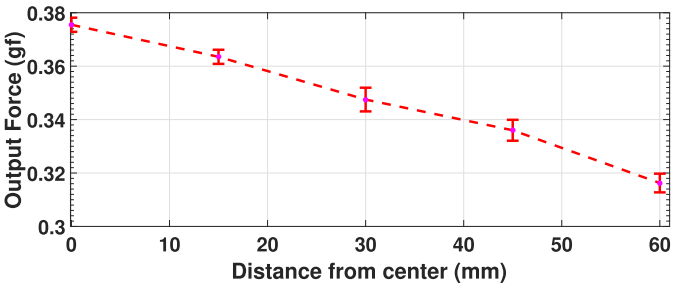

Fig. 5. Output gf value as a function of the distance from the center. The values are averaged over the sample for the four directions around the center. The error bars show the standard deviation.

third-order polynomial for different frequencies and i represents the corresponding frequency.

C. Effect of Deviation From Center

In order to judge the sole effect of the distance from the center on the strength of the focal point, all other parameters were kept constant. The input command value, frequency, and height from the device were 2, 240 Hz, and 200 mm, respectively. The focal point was rendered in all four directions away from the center at a maximum distance of 60 mm with a step size of 15 mm.

The result is shown in Fig. 5. It can be seen that the pressure strength decreases monotonically as focal points move away from the center. It was also noted that the overall trend in all four directions remained the same (see the standard deviation bars).

In order to predict the value of force at an arbitrary location in xy plane, we used a third-order polynomial regression model for the interpolation. The model takes the Euclidean distance of focal point from the origin as an input, and provides the maximum possible output force at that particular point. The regressed function is

$$xy_{\max}(d) = 2.71 \times 10^{-08} d^3 - 1.07 \times 10^{-5} d^2 - 5.05 \times 10^{-5} d + 0.4152 \quad (2)$$

where d is the Euclidean distance of the focal point from center, and $xy_{\max}$ is the maximum output force when height is 200 mm and frequency is 240 Hz.

D. Effect of Height

A similar measurement experiment was conducted to see the effect of height of a focal point. As shown in Fig. 6, the output gf

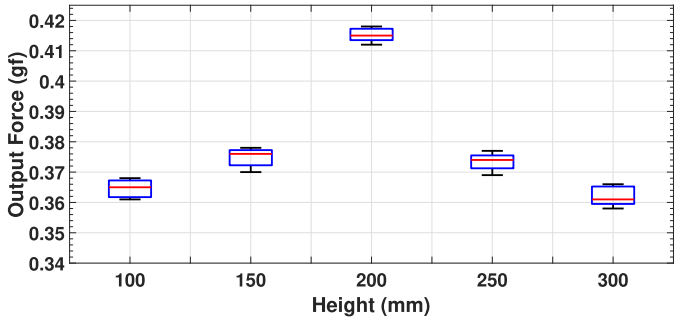

Fig. 6. Effect of height measured at 240 Hz frequency and at the center.

increases as we move the height of focal point up to 200 mm, and after that it starts to decrease. For the interpolation, a second-order polynomial regression model is used to fit the output gf data measured at different positions along z-axis direction (height). The model and the coefficients are as follow:

$$z_{\max}(z) = -1.02 \times 10^{-5} z^2 + 0.0044z + 0.485 \quad (3)$$

where z is the height in millimeters and $z_{\max}$ represents change in output gf.

IV. EXPERIMENT 2

In the second experiment, the mapping from gf to the perceived magnitude of the pressure under different frequency values are formulated through a series of psychophysical experiments. In order to reveal the whole mapping, we first find the minimum perceivable force (or AL) for each frequency. Then, the mapping over the threshold level (supra-threshold range) is estimated through magnitude estimation experiment.

A. Absolute Threshold

a) Participants: A total of 12 participants (four females and eight males) took part in this experiment. Their ages ranged from 23 to 34 years and they reported no disabilities.

b) Experimental Setup: The parameters which were kept constant during this experiment were—the height of focal point at 250 mm and the xy position at the center of device. The focal point was rendered with varying intensity and frequency values. The different rendering frequencies were (40, 80, 120, 160, 240, and 320 Hz), and the input command intensity values of the device were varied from 0 to 2. In this experiment, the stimuli were rendered at the participants' index finger. Fig. 7 shows the experimental setup.

c) Procedure: The design of the experiment was based on the adaptive method with staircase procedures. We used one up and one down method which estimates 50 percentile of a psychometric function. There were two different starting points of the staircase procedure—staircase A (odd numbered trials) where presenting stimuli start from very high intensity and staircase B (even numbered trials) begin with perceptually low stimulus. In both staircases, the intensity of the next presenting stimulus increases in case of a participant's "yes I feel" answer, and it decreases for "no, I do not feel" answer. This process

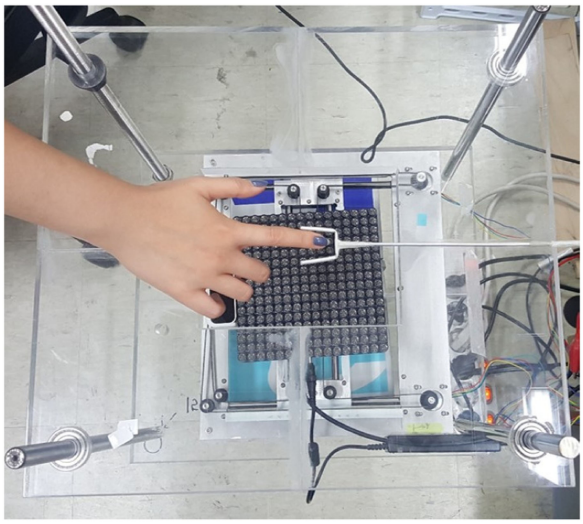

Fig. 7. Experimental setup for AL and perceived magnitude.

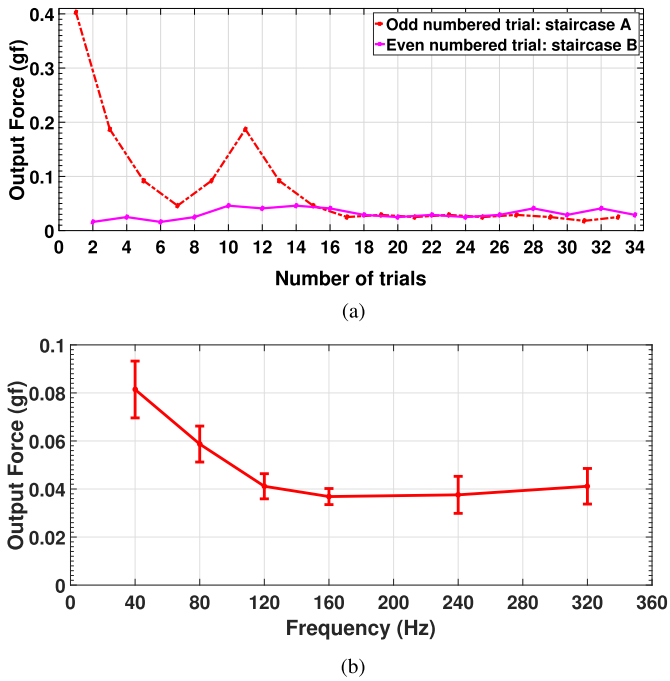

Fig. 8. Results of the AL measurement. (a) An Example: AL measurement result for 80 Hz frequency. (b) AL values for all frequencies.

continued until eight reversals occurred for each of the series. An adaptive step size was also considered. In the beginning the step size was 3 dB, but after three reversals it was reduced to 1 dB. The mean of the intensity at the point of reversals provided the AL value. This whole process was repeated for six different rendering frequency. During the experiment, all the participants were given regular breaks after each stimulus presentation for about 5 s in order to minimize fatigue and sensory bias.

d) Result: Fig. 8(a) is an example result of the experiment (for 80 Hz frequency at 250 mm height). It can be seen that the staircases converge around a single point after a few reversals and remain at that point. The AL values for all the tested frequencies are provided in Fig. 8(b). It shows that the AL is higher for the low frequencies, then decreases until 160 Hz, remains almost constant up to 240 Hz, and then increases again after that. This result highlights that the most sensitive frequency band is the one between 160 and 240 Hz, which coincides with previous literature [13].

B. Perceived Magnitude

The second experiment aims to measure the relation of the physical pressure strength of the generated focal point and its perceptual intensity. This relation is experimentally estimated using the absolute magnitude estimation paradigm [14].

e) Participants: Another set of 16 participants took part in this paper. Ages of the subjects ranged from 24 to 32 years. None of the participants reported any disabilities.

f) Stimuli: The same experimental setup as the AL experiment was used. As the presented stimuli, the gf values were varied with a step size of 1 dB between two consecutive values. Note that actual command to the device was the input command intensity associated to the corresponding gf. The input command levels below AL value were discarded for each frequency. The experiment consisted of 63 conditions—combinations of six frequency values (40, 80, 120, 160, 240, and 320 Hz) and about 7–10 intensity values depending on the AL. Each condition was performed twice.

g) Procedure: All participants went through a 5-min practice session. The stimulus in the form of a focal point was presented to a user for about 2 s. Similar to the previous experiment, 5-s breaks were given to the participants between consecutive stimuli presentations. The participants were asked to rate the perceived magnitude of the stimulus on a free scale.

h) Data Processing: The result of this experiment was in the form of perceived magnitude values associated with different gf values for different frequencies. Every participant's data was normalized separately for each frequency. First of all, geometric mean for each subject (and each frequency) was calculated. Afterward, a grand geometric mean was calculated from the individual geometric means for each frequency. Normalization factor was calculated by taking ratio of grand geometric mean to the individual geometric means. Normalization was done by multiplying each participants' response with the corresponding normalization factor. Due to difference in individual sensitivity, some participants gave "zero" response for intensities in near-threshold level. These intensity levels were not considered.

i) Results: The estimated perceived magnitude is presented in Fig. 9(a)–(f) for each frequency. In each graph, the values of perceived magnitude are represented by blue dots along with the error bars which show the standard deviation. From the AL experiment we concluded that the sensitivity of the 240 and 320 Hz frequencies was higher than other frequencies. It was also observed that these two frequencies provided higher perceived magnitude for corresponding values of gf as compared to other frequencies.

For rendering purpose, it was necessary to find a continuous relation between perceived magnitude and the gf value of the

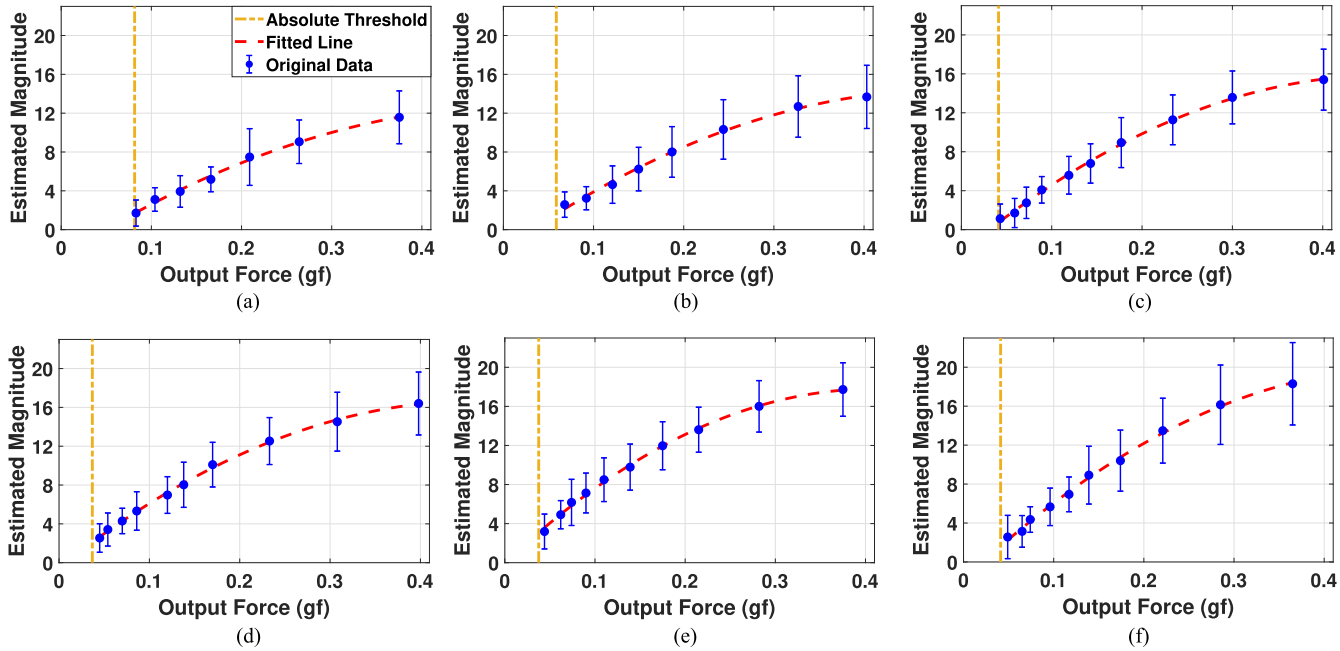

Fig. 9. Measured perceived magnitude for each frequency. (a) 40 Hz. (b) 80 Hz. (c) 120 Hz. (d) 160 Hz. (e) 240 Hz. (f) 320 Hz.

TABLE II
COEFFICIENT VALUES FOR (4)

i (Hz)	P_i	Q_i	S_i	R_i^2
320	-88.569	87.839	-1.849	0.96
240	-106.14	86.977	-0.029	0.92
160	-79.730	74.063	-0.512	0.91
120	-81.745	77.100	-2.307	0.89
80	-66.499	66.257	-2.069	0.86
40	-57.066	59.836	-2.806	0.78

focal point. This relation was modeled using a second-order polynomial model shown in Fig. 9 by a red dashed line. The equation for the polynomial model is provided as

$$\mathrm{PM}_i = P_i f_g^2 + Q_i f_g + S_i \tag{4}$$

where PM is the perceived magnitude, f_g represents the value of gf and P_i, Q_i, and S_i are the coefficient of the second-order polynomial model. The values of the coefficients and the R^2 for each frequency are reported in Table II.

V. TRANSPARENT RENDERING ALGORITHM

According to the data from previous section, it is observed that the finally rendered perceptual strength of a pressure varies not only with the input command intensity but also with the variation in various parameters. The goal of our transparent rendering is to compensate the effect of these parameters on the perceived magnitude, allowing designers to provide an easy and stable control of perceptual intensity without considering the configuration of the physical parameters. Our approach is a measurement-based one where the mapping functions from the command intensity to the perceived intensity are empirically estimated from the data, which is, to our knowledge, the only practical solution.

One of the practical issues of this approach is that if the dimension of input space increases, it becomes very time consuming and sometimes becomes nearly impossible to measure data for every possible combination of the inputs. In our case, we have four-dimensional input which is already the case of this difficulty. Our approach to overcome this is, instead of covering the whole input space with actual measurement data, we only measure multiple representative lines in the input space, capture the trend of it, and interpolate or extrapolate based on the captured trend.

In the Experiment 1, we have formulated the effect of command intensity for different frequency values at a single fixed position (250 mm height, 0 deviation from the center). Similarly, we see the effect of height at a single frequency, at 0 deviation from the center, and at the maximum command intensity. The trend of the deviation from center parameter is also watched only at a fixed height, frequency, and command intensity.

In order to estimate the mapping function for the area of input space other than these lines, we made a couple of assumptions as follows. First, the trend of effect of input command intensity is preserved over different height and different deviation from center. Second assumption is that the trend of effect of the height changes is also preserved over different intensity, frequency, and the deviation from center. In addition, the effect of the deviation from center is also kept over the other parameters. We empirically proved the correctness of this assumption with errors of which the magnitude is mostly less than the difference threshold of human vibration perception.

Under these assumptions, we predict an input command intensity that can provide a desired output gf value for an arbitrary perceived magnitude value as follows. Once the desired

TABLE III
THIRD-ORDER POLYNOMIAL COEFFICIENTS FOR (5)

i [Hz]	A_i	B_i	C_i	D_i	R_i^2
320	34.01	-25.70	8.99	0.32	0.96
240	31.35	-24.05	8.65	0.31	0.97
160	32.20	-25.77	8.98	0.29	0.97
120	21.94	-18.94	7.81	0.34	0.97
80	29.37	-23.99	8.70	0.28	0.98
40	0	0	3.41	0.59	0.92

perceived magnitude is determined by stimuli designer (along with desired frequency), this desired magnitude can be converted into gf using the inverse of (4).

If the parameter configuration is 0, 200 mm for lateral deviation and height, respectively, then this gf value can be directly inserted into the inverse of (1) yielding the desired intensity I. The inverse of (1) can be derived from data by

$$I_i = A_i \mathrm{gf}^3 + B_i \mathrm{gf}^2 + C_i \mathrm{gf} + D_i \tag{5}$$

where A, B, C, and D are the coefficients of the third-order polynomial for different frequencies, and i represents the corresponding frequency. The values for the coefficients for each i are provided in Table III.

However, the estimation becomes invalid if the position of the focal point deviates from (0, 200 mm). In this case, by our assumption (the trend of intensity effect is preserved over height and lateral deviation), I can be still estimated using (5) by inputting a modified gf that is normalized by the effect of height and lateral deviation. Let this normalization scaling factor be F, We can generalize the normalized factor as $\mathrm{gf}_{\mathrm{fact}}$ by directly multiplying it with gf value. The relation can be observed as

$$\mathrm{gf}_{\mathrm{fact}} = \mathrm{gf} F, \tag{6}$$

Now the factor $\mathrm{gf}_{\mathrm{fact}}$ can be substituted in (5) to generate the new desired intensity. In (7), the required relation is established.

$$I_{\mathrm{adj}} = A_i \mathrm{gf}_{\mathrm{fact}}^3 + B_i \mathrm{gf}_{\mathrm{fact}}^2 + C_i \mathrm{gf}_{\mathrm{fact}} + D_i \tag{7}$$

where I_{adj} is the adjusted command intensity that is required to produce the desired output gf under the influence of normalization factor F. As we have already observed, all the parameters partially influence the output gf so we can represent F as a combination of partial factors as follow:

$$F = F_{xy} F_z \tag{8}$$

where F_{xy} is for the effect of distance from center F_z is for the effect of height.

In (2), we formulated the factor $xy_{\max}$ which affects the output gf at the position of the focal point in the xy plane. We can discern that output force of the focal point depletes as we deviate from the center of the device, as shown in Section III. By using (2), we can formulate the factor xy_{fact} by taking the ratio of maximum output force at 0 mm to the output force at the Euclidean distance (d) of the focal point from center as

$$F_{xy} = xy_{\max}(0)/xy_{\max}(d). \tag{9}$$

Similarly, the factor F_z can also be formulated in the same way by taking the height (h) of the focal point from the surface of the device. Mathematically, we can represent the relation using (3) as

$$F_z = z_{\max}(200)/z_{\max}(h). \tag{10}$$

Finally, (7) provides us the dynamically changing command intensity at every point to maintain a fixed perceived magnitude.

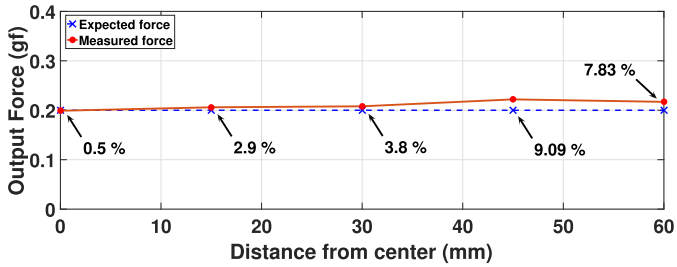

Fig. 10. Expected force values versus measured force values at different locations in the *xy* plane. The error values show the relative error.

VI. EVALUATION

In this section, the evaluation of our rendering algorithm is performed through two experiments. We first test the rendering results that went through our algorithm to check if the rendered pressure remains constant in case of constant desired pressure with different parameters. In the second experiment, a psychophysical experiment is performed to check the performance of the algorithm in perception domain.

A. Measurement Experiment

An experiment was designed to check the accuracy of the rendered output force with varying distance from center. The output was measured with the setup used in the previous section. The algorithm was programmed to render focal points with fixed output force of 0.2 gf at a height of 300 mm from the surface of the device with the frequency of 240 Hz, and the focal points moved from the center to a single direction (positive y) away from the center. A reading was taken at a step size of 15 mm up to a maximum distance of 60 mm.

Fig. 10 shows the results. There are slight errors between the desired pressure and the measured value, which increases as the focal point moves away from the center. The total root-mean-square error is 0.013, while the average error is 6.49%. Note that this amount of error is not perceptually significant according to human pressure just noticeable difference (about 10%) [15], [16].

B. Psychophysical Experiment

The main goal of transparent rendering is to get identical perception of the rendered stimulus with a given constant perceived magnitude regardless of rendering parameters. In order to validate this, a psychophysical experiment was designed to examine how the actual perceived magnitude changed when keeping the desired magnitude constant.

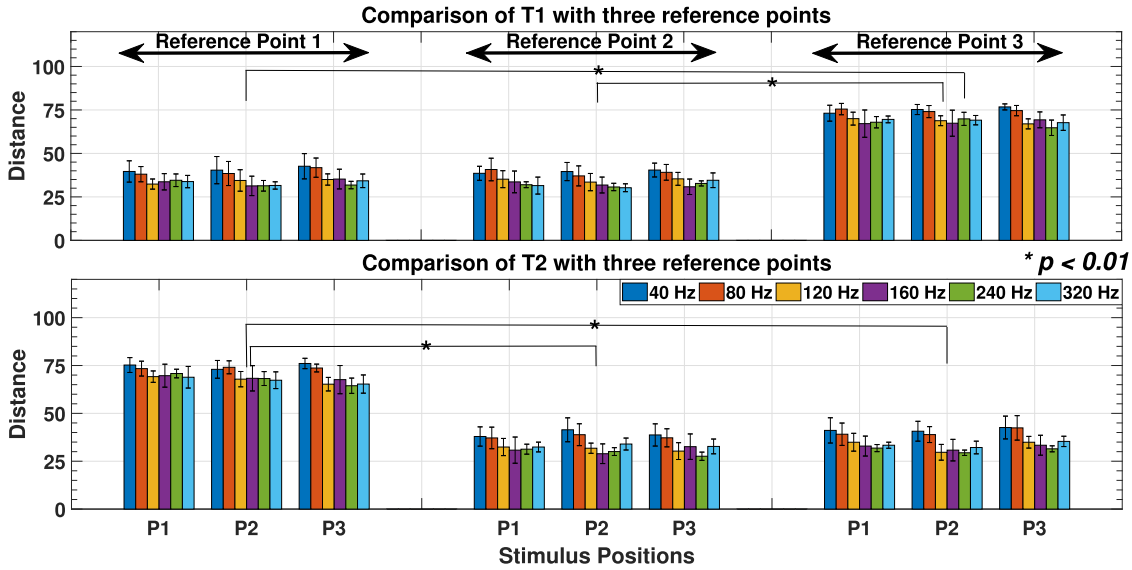

Fig. 11. Perceptual difference between test stimuli (T1 and T2) and reference stimuli (R1, R2, and R3).

j) Participants: Another group of 16 participants (one female and 15 males) took part in this experiment. Their ages ranged from 23 to 31 years, and they reported no disabilities. Additionally, all the participants were provided monetary compensation for taking part in the experiment.

k) Stimuli and Procedure: The same experimental setup and range of frequencies was used as in Section IV. However, the stimuli were rendered in three different positions P1, P2, and P3 in order to check the effect of perceived magnitude in different positions. The coordinates associated with P1, P2, and P3 were (30, −20, 200 mm), (0, 50, 200 mm), and (30, 30, 200 mm), respectively. Each stimulus was presented for 2 s during experiment.

The experiment consisted of two test stimuli T1 and T2 with perceived magnitude of 6 and 10, respectively, with six different frequencies. There were three reference stimuli R1, R2, and R3 with perceived magnitude of 4, 8, and 12 rendered with fixed frequency of 240 Hz. Here we know that T1 has equal distance from R1 and R2 and has maximum distance from R3. On the other hand, T2 has same distance with R2 and R3, and it is at maximum distance from R1. It was required to check if a stimulus with fix perceived magnitude can represent same perception for all frequencies. In order to validate these facts, all the participants were presented with a pair of test and reference stimuli and were asked to rate their difference of strength on a scale of 0–100. There were a total of 108 pairs (combination of six frequencies, three positions, two test, and three reference stimuli). The participants were given 5-s breaks between consecutive stimuli presentations. All the pairs were rendered randomly in three different positions. Each participant went through a 5-min practice session.

l) Data Analysis and Results: The result of the experiment was obtained by averaging all users responses for each pair. The results, shown in the Fig. 11, are representing the perceptual distance of test stimuli with reference stimuli. In the results of our experiment, we observed the expected behavior

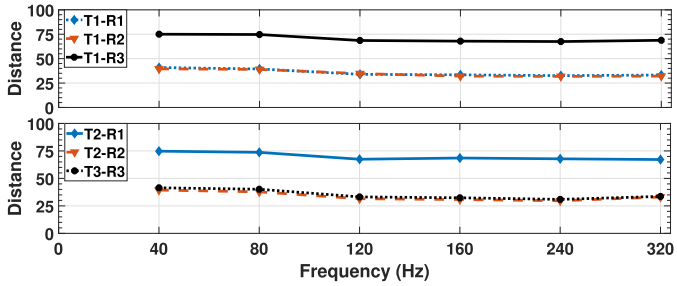

Fig. 12. Data points show the mean value of the distances measured at P1, P2, and P3 for each frequency.

as the user rated first test stimulus for each frequency at almost equal distance from first two reference stimuli i.e., 4 and 8 and farther from the third reference stimulus i.e., 12. On the other hand, participants observed second test stimulus T2 at minimum distance with second and third reference stimuli (R2 and R3) and farther from the first stimulus R1. Furthermore, statistical analysis was done on the experimental data by using ANOVA test. For T1, R1, and R2 were found to be significantly different ($p < 0.01$) from R3. In case of T2, R2, and R3 were found to be significantly different ($p < 0.01$) from R1. Result shows that the average distance response of the stimulus with two frequencies 40 and 80 Hz was higher than the other frequencies. Whereas the stimuli with other four frequencies were perceived at the same level.

In order to find the quantitative relation between the measured perceptual distances, we calculated the ratio among the distance values for each frequency. First, we calculated the mean value (P1, P2, and P3) of the distances measured between reference points R1, R2, and R3 and test point T1 and T2 (shown in Fig. 12). Second, we computed the ratio between those mean values for each frequency i.e (40, 80, 120, 160, 240, 320) Hz. For T1, the ratios among distances R2/R1, R3/R1, and R3/R2

TABLE IV
RATIO COMPARISON BETWEEN REFERENCE POINT R1, R2, AND R3 FOR TEST POINT T1 AND T2

Ratios Comparison		Frequency 40	80	120	160	240	320
T1	R2-R1	0.97	0.99	1.02	0.96	0.98	0.97
	R3-R1	1.84	1.89	2.02	2.03	2.07	2.07
	R3-R2	1.90	1.92	1.98	2.12	2.12	2.14
T2	R1-R2	1.90	1.95	2.14	2.23	2.29	2.03
	R1-R3	1.80	1.84	2.03	2.12	2.19	2.00
	R2-R3	0.95	0.94	0.95	0.95	0.96	0.98

are shown in Table IV. Here we can observe that T1 has almost same distance from R1 and R2 as their computed ratio is around 1. On the other hand, the ratios of distances T1 and R3 with respect to R1 and R2 are between 1.8–2.2 which validates T1 has larger distance with R3 then R1 and R2. Similarly, for T2 the ratios among distances R1/R2, R1/R3, and R2/R3 are given in the Table IV as well. Here, T2 has the similar distance with R2 and R3 and larger distance with R1.

VII. DISCUSSION

As discussed earlier, the force output of the UltraHaptics device decreases as we move away from the center in a direction parallel to the plane of the device. Similarly, the force output also changes with respect to height from the device and the operation frequency. However, in certain scenarios we are required to render volumetric object with an output force that provides a constant perceived magnitude to the user. This is important because in real world a given surface exhibits the same physical characteristics across its totality. To this end, the transparent rendering algorithm ensures that the output perceived magnitude remains nearly constant across a volumetric object. From Fig. 10 it is evident that the transparent rendering algorithm can successfully render focal points for a given perceived magnitude by dynamically changing the output force value.

The main strategy behind maintaining a fixed perceived magnitude is to somehow adjust the input command value at different locations. For instance, while moving away from center the command value needs to be increased by a certain factor to maintain transparency during rendering. However, the maximum input command value is capped at 2 and this value translates into gradually decreasing maximum force as we move away from the center. This means that we are unable to produce a given force at a farther distance equal in magnitude to the maximum force at the center. This phenomenon acts as a limiting factor on the maximum constant output force that can be rendered across a volumetric object. The maximum force (against input command value of 2) available at the boundaries of the object is less as compared to the center. Thus, the object can only be rendered with a constant perceived magnitude associated with farthest point on its surface. For example, a volumetric surface centered at zero extends 40 mm along x and y directions. Let's assume that the maximum output force at center and 40 mm away from the center is 0.2 and 0.15 gf against input command value 2, respectively. In this case, the maximum constant output force that can be rendered across the whole object is 0.15 gf. Thus, the limiting factor in this case is the maximum force available at the location farthest from the center.

One of the limitations of the approach is that for different ultrasonic-based haptic devices, the measurement experiment reported in Section III should be redone. However, the two-step approach used in this paper is the result of our effort to minimize the effect of this limitation. By separating physical measurement step from user-involved psychophysical study, the only step that should be redone is the physical measurement step (from command intensity to gf). We speculate that this is the least process in order for incorporating device-dependent characteristics (e.g., different kinds of command unit, intensity changing characteristics, and so on). For instance, in case of a device where input voltage to the transducers is controlled, the relationship between input voltage and output force can be re-measured and inserted to our algorithm, and then the transparent rendering is achieved.

VIII. CONCLUSION

In this paper, we designed an algorithm that can maintain transparency between the input and output of the an ultrasound-based haptic device. To achieve this goal, we performed some experiments to establish a relationship between the input parameters and the actual perception of the focal point. The derived algorithm can help minimize the effect of device dynamics providing consistent output force at the desired focal point.

REFERENCES

[1] S. Coren, L. M. Ward, and J. T. Enns, *Sensation and Perception*. New York, NY, USA: John Wiley & Sons, 2003.
[2] H. Culbertson, J. Unwin, and K. J. Kuchenbecker, "Modeling and rendering realistic textures from unconstrained tool-surface interactions," *IEEE Trans. Haptics*, vol. 7, no. 3, pp. 381–393, Jul./Sep. 2014.
[3] A. T. Maereg, E. L. Secco, T. F. Agidew, R. Diaz-Nieto, and A. Nagar, "Wearable haptics for VR stiffness discrimination," presented at the Euro. Robot. Forum, Edinburgh, U.K., Mar. 22–24, 2017.
[4] F. Arafsha, L. Zhang, H. Dong, and A. E. Saddik, "Contactless haptic feedback: State of the art," in *Proc. IEEE Int. Symp. Haptic, Audio Vis. Environ. Games*, Oct. 2015, pp. 1–6.
[5] H. Lee *et al.*, "Mid-air tactile stimulation using laser-induced thermoelastic effects: The first study for indirect radiation," in *Proc. IEEE World Haptics Conf.*, Jun. 2015, pp. 374–380.
[6] R. Sodhi, I. Poupyrev, M. Glisson, and A. Israr, "AIREAL: Interactive tactile experiences in free air," *ACM Trans. Graph.*, vol. 32, no. 4, pp. 134:1–134:10, Jul. 2013.
[7] L. Gavrilov, E. Tsirulnikov, and I. a. I. Davies, "Application of focused ultrasound for the stimulation of neural structures," *Ultrasound Med. Biol.*, vol. 22, no. 2, pp. 179–192, 1996.
[8] T. Hoshi, M. Takahashi, T. Iwamoto, and H. Shinoda, "Noncontact tactile display based on radiation pressure of airborne ultrasound," *IEEE Trans. Haptics*, vol. 3, no. 3, pp. 155–165, Jul./Sep. 2010.
[9] G. Korres and M. Eid, "Haptogram: Ultrasonic point-cloud tactile stimulation," *IEEE Access*, vol. 4, pp. 7758–7769, 2016.
[10] T. Carter, S. A. Seah, B. Long, B. Drinkwater, and S. Subramanian, "Ultrahaptics: Multi-point mid-air haptic feedback for touch surfaces," in *Proc. 26th Annu. ACM Symp. User Interface Softw. Technol.*, New York, NY, USA, 2013, pp. 505–514.
[11] G. Korres and M. Eid, "Characterization of ultrasound tactile display," in *Proc. Int. Conf. Human Haptic Sens. Touch Enabled Comput. Appl.*, 2016, pp. 78–89.
[12] J. Ryu, J. Jung, S. Kim, and S. Choi, "Perceptually transparent vibration rendering using a vibration motor for haptic interaction," in *Proc. 16th IEEE Int. Symp. Robot Human Interactive Commun.*, Aug. 2007, pp. 310–315.

[13] S. J. Bolanowski Jr, G. A. Gescheider, R. T. Verrillo, and C. M. Checkosky, "Four channels mediate the mechanical aspects of touch," *J. Acoustical Soc. Amer.*, vol. 84, no. 5, pp. 1680–1694, 1988.
[14] J. Zwislocki and D. Goodman, "Absolute scaling of sensory magnitudes: A validation," *Perception Psychophys.*, vol. 28, no. 1, pp. 28–38, Jan. 1980. [Online]. Available: https://doi.org/10.3758/BF03204312
[15] X.-D. Pang, H. Z. Tan, and N. I. Durlach, "Manual discrimination of force using active finger motion," *Perception Psychophys.*, vol. 49, no. 6, pp. 531–540, 1991.
[16] L. A. Jones, "Matching forces: constant errors and differential thresholds," *Perception*, vol. 18, no. 5, pp. 681–687, 1989.

Ahsan Raza received the B.S. degree in computer engineering from the University of Engineering and Technology (UET) Taxila, Pakistan, in 2015. Currently, he is working toward the Ph.D. degree in computer engineering with the Department of Computer Science and Engineering, Kyung Hee University, Namyangju, South Korea.

His research interests include mid-air haptic feedback, haptic guidance and perception, and psychophysics.

Waseem Hassan received the B.S. degree in electrical engineering from the National University of Science and Technology, Islamabad, Pakistan, and the M.S. degree in computer engineering from Kyung Hee University, Namyangju, South Korea. Currently, he is working toward the doctoral degree in computer engineering with the Department of Computer Science and Engineering at Kyung Hee University.

His research interests include psychophysics, and haptic texture perception, and augmentation.

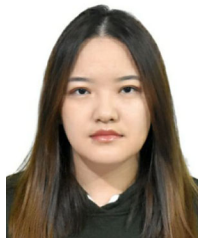

Tatyana Ogay received the B.S. degree in informatics and information technologies from the Tashkent University of Information Technologies, Tashkent, Uzbekistan, in 2015, and the M.S. degree in computer science and engineering from Kyung Hee University, Namyangju, South Korea, in 2018. Currently, she is working toward the Ph.D. degree in computer engineering with the Department of Computer Science and Engineering, Kyung Hee University.

Her research interests include haptic rendering, nonlinear object deformation in augmented environment, and human computer interaction.

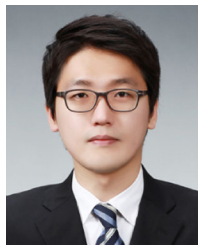

Inwook Hwang received the B.S. and Ph.D. degrees in computer science and engineering from the Pohang University of Science and Technology, Pohang, South Korea, in 2006 and 2013, respectively.

He is a Senior Researcher with Software and Contents Research Laboratory, Electronics and Telecommunication Institute, Daejon, South Korea. His main research interests include haptic perception, haptic rendering, and multimodal user interfaces.

Seokhee Jeon received the B.S. and Ph.D. degrees in computer science and engineering from the Pohang University of Science and Technology, Pohang, South Korea, in 2003 and 2010, respectively.

He was a Postdoctoral Research Associate at Computer Vision Laboratory, ETH Zurich, Zurich, Switzerland. In 2012, he joined as an Assistant Professor with the Department of Computer Engineering, Kyung Hee University, Namyangju, South Korea. His research interests include haptic rendering in an augmented reality environment, applications of haptics technology to medical training, and usability of augmented reality applications.